REPORT NO.
UCB/SEMM-92/20

STRUCTURAL ENGINEERING
MECHANICS AND MATERIALS

EXTENSIONAL BEHAVIOR OF MULTI-CRYSTALLINE BEAMS

BY

MAURO FERRARI
AND
CHUN-LIANG LIN

JUNE 1992

DEPARTMENT OF CIVIL ENGINEERING
UNIVERSITY OF CALIFORNIA
BERKELEY, CALIFORNIA

EXTENSIONAL BEHAVIOR OF MULTI-CRYSTALLINE BEAMS

Mauro Ferrari* & Chun-Liang Lin
Department of Civil Engineering
* also, Department of Materials Science and Mineral Engineering
University of California, Berkeley, CA 94720

ABSTRACT

The problem of simple extension of a multicrystalline silicon beam is discussed, by numerically analyzing the 3-D elastic fields as functions of the grain morphological and orientational portraits. These are computer-generated in accordance with assigned probability density functions. Macroscopic quantities(as centerline elongation) and the maxima of local fields (stresses, lateral boundary displacements) are correlated to distributional parameters, and are compared with those predicted by the theory of homogenization of textured polycrystals. The most significant deviations from the classic beam response are the large transverse displacements, and the moderate cross-sectional stresses, associated with certain microdistributions. The numerical analysis is performed with the software ABAQUS on a DEC 5000 workstation.

INTRODUCTION

Standard beam and plate theories are based on the assumptions on material isotropy and homogeneity. Such assumptions are generally justifiable for polycrystalline aggregates, i.e. bodies for which the typical grain-to-structural ratio is very small, and the number of constituent crystals is consequently very large. However,these assumptions are inappropriate, for the analysis of structures consisting of a limited number of grains. Such arrangements, which have been dubbed 'multicrystalline', need in general be analyzed as composite structures, with each grain being a uniform, anisotropic substructure, surrounded by typically inhomogeneous grain boundary regions.

While some advances in the analysis of miniaturized structures (MEMS) have been accomplished through the anisotropic composite structure model [1], such approach is clearly prohibitive, at the current technological stage, in view of the still large number of component crystals present in such objects. On the other hand, the typical cross section of a micro-scale structure may contain very few grains, or possibly only one, thus rendering the use of

standard structural theories open to questioning.

The need thus arises to develop a structural theory that incorporates grain-level effects, while maintaining macroscopic predictive capabilities and a manageable format. Toward this goal, the appropriateness of both stochastic and deterministic methods are currently under investigation.

On the deterministic side, a viable approach consists of obtaining the homogenized (effective) material response as a function of the grain distributions and properties, and then applying the conventional analytical or numerical methods for homogeneous structures. Such technique yields the average mechanical fields only, but is in principle applicable to any partition of the structure into homogenized sub-structures, thus obtaining a closer approximation to the actual elastic fields with each finer re-partitioning [2].

The obvious drawbacks of this technique reside in 1) the difficulty of experimental observation of the local grain distributions, 2) the computational and analytical complexity, 3) the generally unsatisfactory predicting abilities of homogenization theory, and 4) most improtantly, the inability to distinguish among microdistributions that result in identical averages, thus ignoring the local fluctuations that are typically responsible for failure.

When integrated with sufficient material characterization, the use of the stochastic finite element method offers valuable information for the overcoming of the drawbacks 3 and 4. Such methods have been applied in [3] for the analysis of flexural two-dimensional beams to yield the expected stresses and their fluctuations in the presence of different, computer-simulated, equiprobable microdistributions.

In this paper, the three-dimensional analysis of extensional polysilicon elements is undertaken, using the software ABAQUS [4] on beams with simulated grain distributions. The objective of this work is the assessment of the material and structural domains in which the mean field values are significant for the purposes of analysis and design. In particular, the scatter of local and global quantities is investigated, as a function of the beam geometry, in an effort to identify the domain of validity of the homogenization/standard theory approach. The local quantities considered include the maximum stresses and transverse displacements, while the global ones include the centerline axial displacements (and thus the effective longitudinal modulus). The accuracy of the constant field homogenization approaches of Voigt/Reuss, and of the assumption of overall isotropy are also discussed.

HOMOGENIZATION TECHNIQUES

Consider a monophase polycrystalline structure, consisting of perfectly bonded grains of stiffness $\underline{c}^c$, with inverse $\underline{s}^c$. The grains are oriented according to the orientation probability density function f(g) where g is used to denote the triad of Euler angles (ψ_1, Φ, ψ_2), defined as in Fig. 1-1, 1-2. The structure is subjected to homogeneous boundary condition, either of the displacement type:

$$\underline{u} = \underline{\varepsilon}^0 \underline{x} \qquad (1)$$

or of the stress type:

$$\underline{t} = \underline{\tau}^0 \underline{n} \qquad (2)$$

Here, $\underline{u}$ is the displacement vector, $\underline{t}$ is the traction vector ,$\underline{n}$ is

the unit normal vector, $\underline{x}$ is the position vector, $\underline{\tau}$ and $\underline{\varepsilon}$ are the stress and strain tensors, and a superscript '0' denotes symmetry, arbitrariness, and spatial homogeneity.

Introducing the orientation dependent strain and stress concentrator tensors $\underline{A}$ and $\underline{B}$, respectively defined as

$$\bar{\underline{\varepsilon}}^c = \underline{A}\,\underline{\varepsilon}^0 \qquad (3)$$

under (1) and

$$\bar{\underline{\tau}}^c = \underline{B}\,\underline{\tau}^0 \qquad (4)$$

under (2), where overbars denote spatial averages at a fixed orientation g, the effective, or average, stiffness and compliance tensors are easily shown to be respectively

$$\underline{C} = \langle\, \underline{C}^c\underline{A} \,\rangle \quad \text{and} \quad \underline{S} = \langle\, \underline{S}^c\underline{B} \,\rangle \qquad (5)$$

Here, the pointed brackets denote the invariant, normalized, texture-weighted orientational averaging:

$$\langle . \rangle \equiv 1/8\pi^2 \int_0^{\pi}\int_0^{2\pi}\int_0^{2\pi} \Pi(.)\, f(g) \sin\phi\, d\psi_1\, d\psi_2\, d\phi \qquad (6)$$

where $\Pi(.)$ is the frame change operator. Thus , the typical element of the tensor $\Pi(.)$ is a linear combination of R-fold products of elements of Euler matrix, R being the tensorial rank of the argument.

For the purpose of computation of the integrals in (5,6) it is convenient to expand the function f(g) in a series of symmetrized, generalized spherical harmonics, and then to truncate this series at the order R. By the central theorem of [5], resting on the equivalence of all representations of the same order of the group of rotations, this procedure does not introduce any further approximation.

The most widely used homogenization approaches consist of taking either $\underline{A}$ and $\underline{B}$ to be equal to the fourth rank tensorial identity, corresponding to the procedures of Voigt and Reuss yielding, respectively:

$$\underline{C}^{Voigt} \equiv \underline{C}^V = \langle\, \underline{C}^c \,\rangle \qquad (7)$$

$$\underline{C}^{Reuss} \equiv \underline{C}^R = \langle\, \underline{S}^c \,\rangle^{-1} \qquad (8)$$

The intrinsic advantage of such approaches, besides their simplicity,resides in the fact that the associated moduli are rigorous upper and lower bounds to the actual effective moduli, respectively.

STOCHASTIC NUMERICAL ANALYSIS

Initially straight three-dimensional beams with square,untapered cross sections were investigated, with span-to-height ratios of 10/3 to 100/3. The beam was subdivided into 3X3X100 = 900 cubic 8-node elements, and subject to unit axial tension on both bases. The finite element mesh is shown in Figure 2-1. The grains were randomly assigned lateral dimensions of 1 to

3 units, and axial dimensions of 1 to 10 units (Fig 2-2).

Each grain was assigned the (cubic) silicon elastic constants C11 = 166 GPa, C12 = 63.8 GPa, C44 = 79.5 GPa, expressed in a natural crystal-fixed frame. The following normalized orientation distribution functions were considered:

$$f(g,\gamma) = (e/\pi)^{1/2}\, G_{\gamma}\, (\Phi)\ \delta(\psi 1)\ \delta(\psi 2) \qquad (9)$$

$$f(g,\gamma) = (e/\pi)^{1/2}\, G_{\gamma}\, (\psi 1)\ \delta(\Phi)\ \delta(\psi 2) \qquad (10)$$

$$f(g,\gamma) = (e/\pi)^{1/2}\, G_{\gamma}\, (\psi 1-\pi/4)\ \delta(\Phi)\ \delta(\psi 2) \qquad (11)$$

$$f(g,\gamma) = (e^4/\pi)^{1/2}\, G_{\gamma}\, (\psi 1)\ \delta(\Phi)\ \delta(\psi 2) \qquad (12)$$

$$f(g,\gamma) = (e^4/\pi)^{1/2}\, G_{\gamma}\, (\psi 1-\pi/4)\ \delta(\Phi)\ \delta(\psi 2) \qquad (13)$$

Where, $G(X) = \mathrm{Exp}(-\gamma X^2)$ and $\delta(x)$ are the Gaussian and Dirac's distribution functions, respectively; $\gamma = 1/(2\sigma^2)$, and σ is the standard deviation [6]. The orientations of the single grains were computer-generated according to (9 - 13).

DISCUSSION

Table 1 shows the percentile error in various quantities, resulting from the use of the isotropic homogenization approaches of Voigt, Reuss, and their tensoral average, for beams with aspect ratio of 100/3, and orientation profile given by (9). This orientation distribution corresponds to cross-sectional misalignment, as shown in Fig. 1-2.

TABLE 1. Relative Error - Texture given by (9)

	Perfect Cubic	Voigt	Reuss	Average
u (0.7662)	0.2%	-21%	80%	29%
E11 (130.51)	-0.2%	27%	-44%	-23%
v (0.278)	0.0%	-39%	143%	51%

Here, u and v are respectively the centerline axial displacement and Poisson's ratio, while E11 is the axial modulus in the longitudinal direction. The figures in parentheses, corresponding to the means of five numerical experiments with identical textural and orientation distribution functions are here taken as reference values.

Table 1 demonstrates the errors associated with the disregarding of the texture - a most common assumption. Errors identical to the third decimal to those exhibited in Table 1, persist for more in-plane misoriented distributions - corresponding to (9) with $\ln\gamma$ up to 1, or standard deviation of $(2e)^{-1/2}$.

For all cases of pure cross-sectional texturing, this numerical analysis exhibits spatial constancy of the longitudinal stress, up to the fourth decimal, and zero non-longitudinal stresses, up to the third decimal. This is in agreement with the expectations, based on the near perfect alignment of the crystals.

The slenderness of the beam was shown to be irrelevant, given the present grain size and orientation distributions, down to aspect ratios of 10/3.

Microbeams with grains with only one cubic axis parallels to the cross-sectional planes (Fig. 1-2) are considered next. The

orientation distributions (9 - 13) are characterized in Table 2, together with the results of the simulations.

Table 2. Simulation Results - Texture given by (9-13), l/d = 100/3

	mean	lnγ	σ	u	E11	v_{12}	v_{13}	Vmax
(9)	Φ 0.0	1	$(2e)^{-1/2}$	0.7662	130.51	0.278	0.278	7.0034E-3
(12)	ψ1 0.0	4	$(2e^4)^{-1/2}$	0.7587	131.80	0.282	0.272	1.1008E-2
(10)	ψ1 0.0	1	$(2e)^{-1/2}$	0.6996	142.67	0.200	0.304	0.1204
(11)	ψ1 π/4	1	$(2e)^{-1/2}$	0.6577	152.10	0.158	0.327	0.1814
(13)	ψ1 π/4	4	$(2e^4)^{-1/2}$	0.5983	167.15	0.075	0.355	1.4937E-2

Here, Vmax denotes the maximum transverse displacement recorded in the simulations.

(12) and (13) represent distributions near perfect alignment, since the corresponding standard deviation is 0.0036. In this context, for (12) the axes of alignment coincide with the structural axes, while for (13) there are skewed by $\pi/4$. Thus, distribution (12) yields the microbeam with the most compliant response, while (13) yields the stiffest one, as verified in Table 2. The axial elastic modulus for (12) is a little larger than that for (9), as the former contains a slight out-of-plane cubic axis misalignment.

For (12) & (13), with corresponding deviation of 0.0036, the maximum longitudinal stress fluctuation is approximately 5%, while the transverse normal stresses and shears reach 6% and 9% of the applied tensile load, respectively. For (10) & (11), with corresponding deviation of 0.4289, the axial stress fluctuations reach 20%, and the peak transverse normal stresses and shears are 17% and 15% of the applied load, respectively. These stresses are caused by the different axial moduli and Poisson's ratios in the same cross section.

The responses of the microbeams with distributions (10) & (11) differ from those of standard tension members, in that large transverse defections are present (see Fig. 3). These are caused by the different axial elongations of crystals in the same cross section, which in turn are the result of the relative crystal misalignment. To confirm this, the special cases of Fig. 4 were analyzed:

Case 1. The structure is divided into 10 equal sections longitudinally. The ψ1 distribution varies from 0 at both ends to $\pi/4$ at center with the increments of $\pi/16$.

Case 2. The structure is divided into three strips vertically. The ψ1 distribution is 0 at one side, $\pi/8$ at the middle, and $\pi/4$ at the other side.

Case 3. The structure is divided into three strips horizontally. The ψ1 distribution is 0 at the top, $\pi/8$ at the middle, and $\pi/4$ at the bottom.

Table 3 shows the results of this analysis.

Table 3. Comparison between (12),(13),and case 1-3

	u	E11	v_{12}	v_{13}
(12)	0.7587	131.80	0.28	0.27
Case 1	0.6791	147.25	0.19	0.31
Case 2	0.7353	136.00	0.17	0.29
Case 3	0.7330	136.43	0.17	0.29
(13)	0.5983	167.15	0.08	0.36

In agreement with the expectations, the longitudinal moduli for the cases 1-3 fall between those for (12) and (13), and the differences in the axial moduli in the cross-sectional element generate large lateral displacements in cases 2 & 3 (Fig. 5 & 6).

CONCLUSIONS

1. Multicrysatlline microbeams characterized by grains with two cubic axes normal to the beam axis exhibit a longitudinal elastic response that is quite independent from the details of the textural and grain morphological distributions, and as thus adequately simulated by homogenization approaches. However, even for these cases the homogenization approaches of Voigt/Reuss are insufficient.

2. Microbeams with grains with a single cubic axis in the cross-sectional planes are longitudinally stiffer than those considered in 1. The stiffest such beam corresponds to perfect alignment of the grains at $\psi 1 = \pi/4$, with a modulus only about 1% smaller than the overall maximal one (E = 169.2 GPa in the cubic diagonal direction).

3. In the simulations, the longitudinal modulus of the stiffest beam was E11 = 167.15 GPa, and associated with it was the highest in-plane coordinate anisotropy (v_{12} = 0.075, v_{13} = 0.355). Conversely, the most compliant beam, corresponding to (9), had E11 = 130.51 GPa and identical Poisson's ratios in the cross-sectional coordinate directions (v = 0.278). By contrast, for a perfect cubic grain, the most compliant responses are found with E11 = 130.58 GPa, and v = 0.278, corresponding to $\Phi = 0$ & $\psi 1 = 0$.

4. Large lateral displacements, variations in the longitudinal stresses, and significant non-longitudinal stresses may be found in a misoriented microbeam in tension, resulting from different axial elongations of adjacent grains. The severity of these phenomena increases with increasing standard deviation in the textural portrait.

REFERENCES

[1] M. Ferrari & M. E. Weber, "Determination of eigenstresses from curvature data", (Materials Research Society 1992 Spring Meeting, april 27 - May 1, 1992, San Francisco, CA. -Symposium Y: Materials for Electromechanical Systems).

[2] D. Mirfendereski & M. Ferrari & A. Der Kiureghian, "Analysis of microfabricated textured multicrystalline beams: I. Homogenization" (Materials Research Society 1992 Spring Meeting, April 27 - May 1, 1992, San, Francisco, CA. -Symposium Y: Materials for

Electromechanical Systems).

[3] D. Mirfendereski & A. Der Kiureghian & M. Ferrari, "Analysis of microfabricated textured multicrystalline beams: II. Stochastic finite element methods." (Materials Research Society 1992 Spring Meeting, April 27 - May 1, 1992, San, Francisco, CA. -Symposium Y: Materials for Electromechanical Systems).

[4] ABAQUS,1989, Hibbit, Karlsson, and Sorensen, Inc. Pawtucket, RI.

[5] M. Ferrari & G.C. Johnson, "On the equilibrium properties of a 6mm polycrystal exhibiting transverse isotropy", Journal of Applied Physics, 63, 9, 4460-4468,1988.

[6] Alfredo H.S. Ang & Wilson H. Tang, 1984, " Probability Concepts in Engineering Planning and Design", Volume 2, pp274-291.

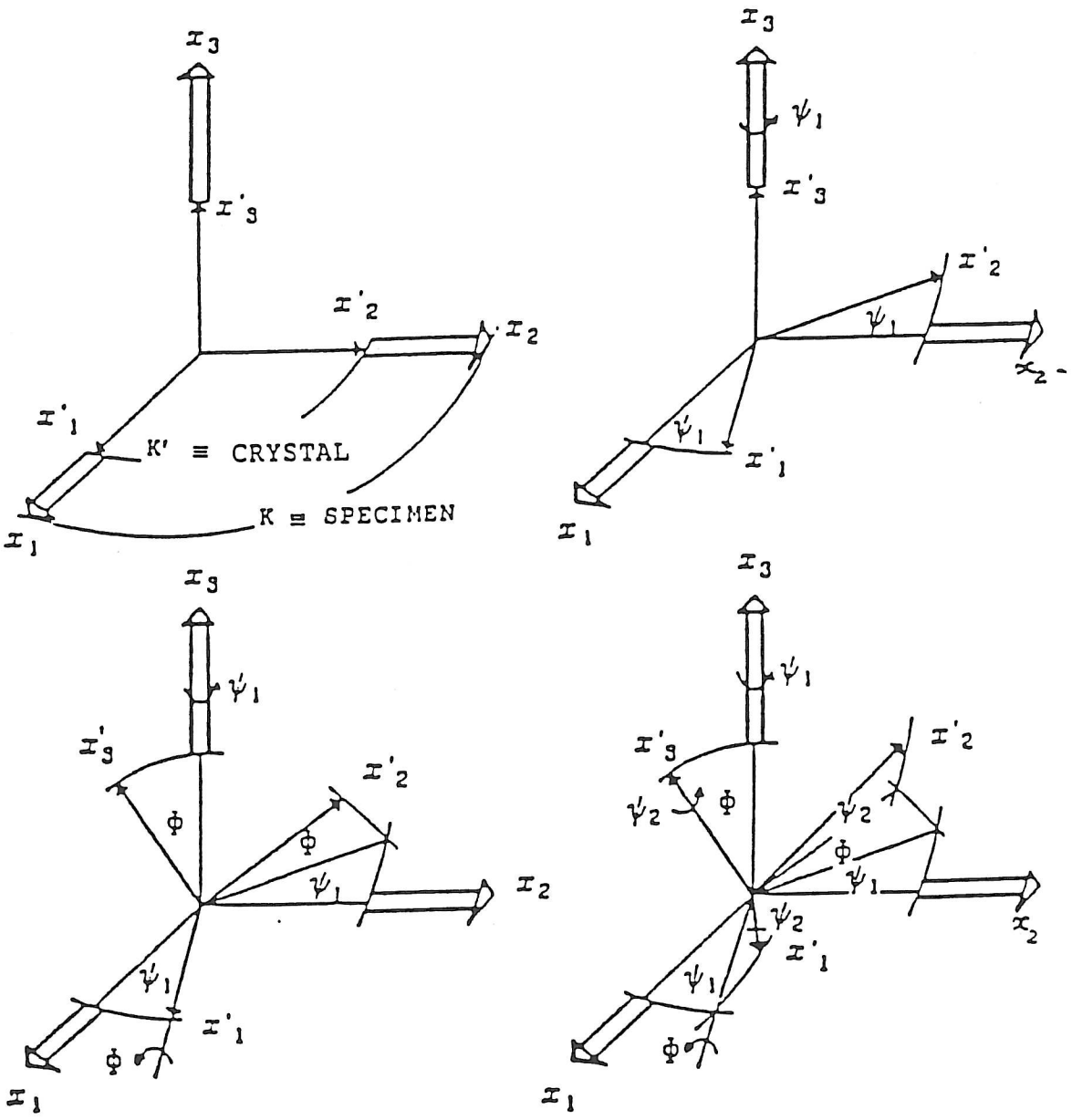

Fig. 1-1 Convention on Euler Angles

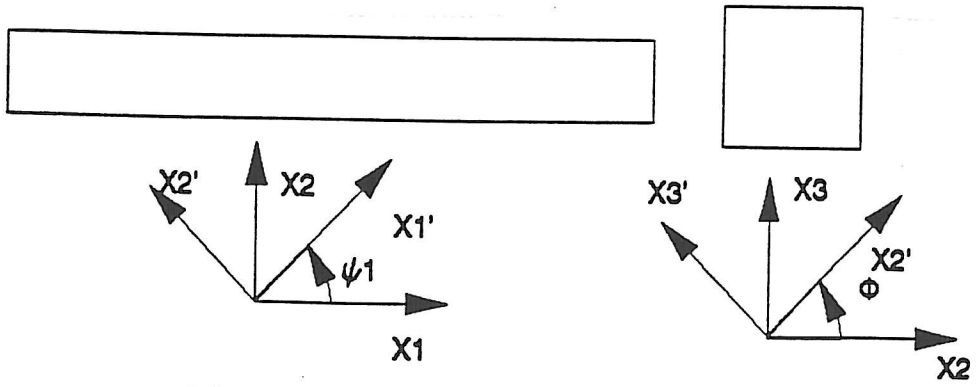

Fig. 1-2 Convention on Euler Angles

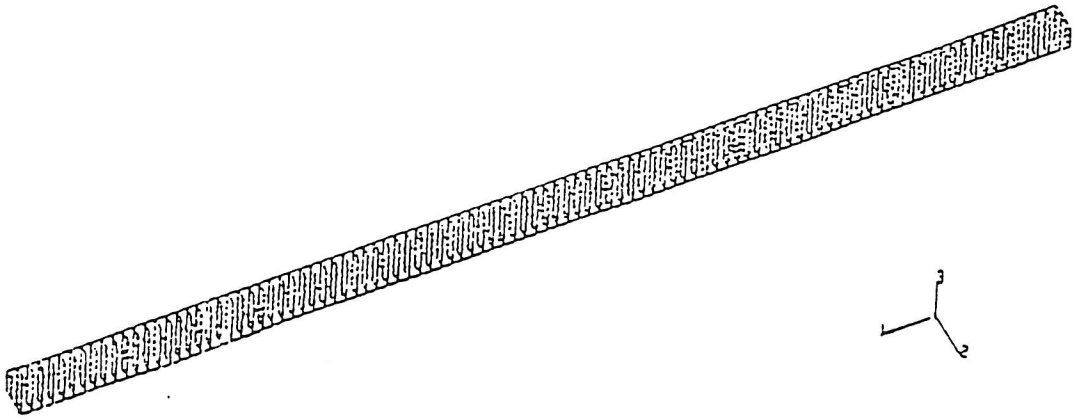

Fig. 2-1 Finite Element Mesh

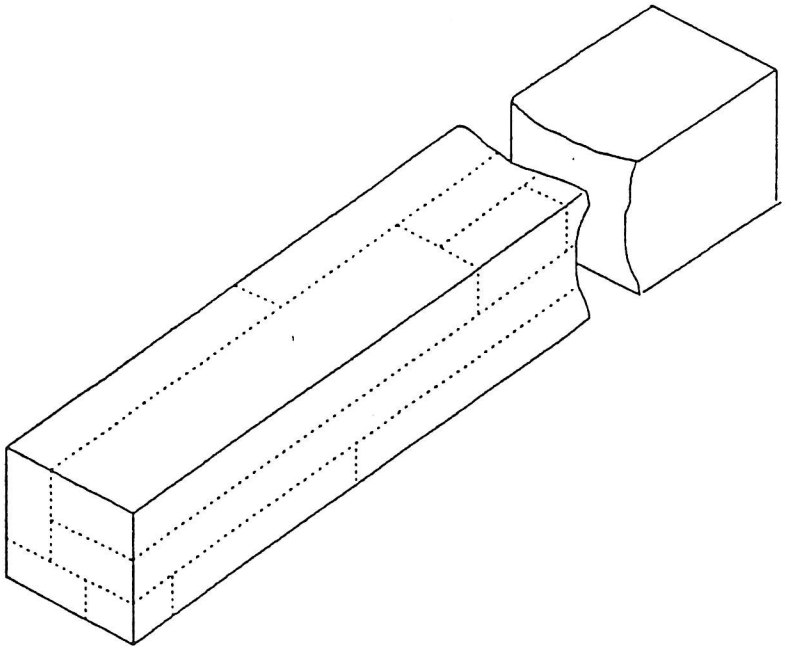

Fig. 2-2 Typical Grain Distribution

Fig. 3 Deformed Mesh for Eq. (10)

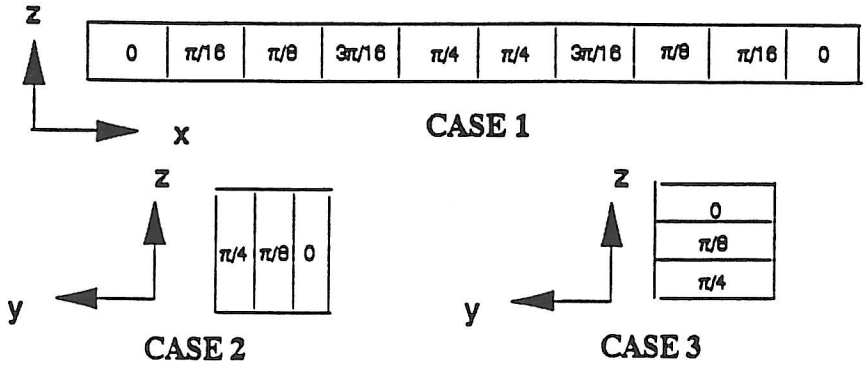

Fig. 4 Orientation Distribution for Cases 1-3

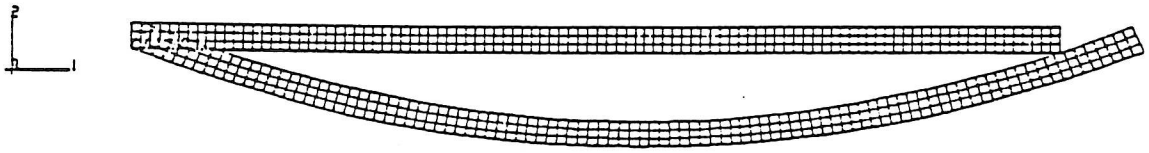

Fig. 5 Deformed Mesh for Case 2

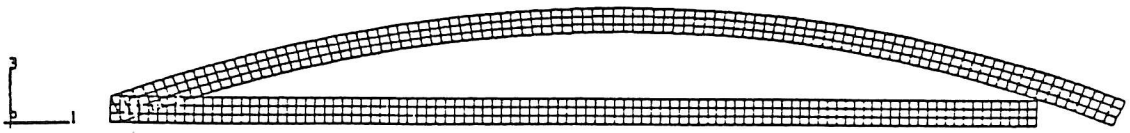

Fig. 6 Deformed Mesh for Case 3